Brief Communications

Axonal Thinning and Extensive Remyelination without Chronic Demyelination in Spinal Injured Rats

Berit E. Powers,[1,3]* Jurate Lasiene,[1,3]* Jason R. Plemel,[4]* Larry Shupe,[2] Steve I. Perlmutter,[2] Wolfram Tetzlaff,[4] and Philip J. Horner[1,3]

Departments of [1]Neurological Surgery, [2]Physiology and Biophysics, and [3]Institute for Stem Cell and Regenerative Medicine, University of Washington, Seattle, Washington 98109, and [4]International Collaboration on Repair Discoveries, Blusson Spinal Cord Center, University of British Columbia, Vancouver, British Columbia V6T 1Z4, Canada

Remyelination following spinal cord injury (SCI) is thought to be incomplete; demyelination is reported to persist chronically and is proposed as a compelling therapeutic target. Yet most reports do not distinguish between the myelin status of intact axons and injury-severed axons whose proximal stumps persist but provide no meaningful function. We previously found full remyelination of spared, intact rubrospinal axons caudal to the lesion in chronic mouse SCI. However, the clinical concept of chronically demyelinated spared axons remains controversial. Since mouse models may have limitations in clinical translation, we asked whether the capacity for full remyelination is conserved in clinically relevant chronic rat SCI. We determined myelin status by examining paranodal protein distribution on anterogradely labeled, intact corticospinal and rubrospinal axons throughout the extent of the lesion. Demyelination was evident on proximal stumps of severed axons, but not on intact axons. For the first time, we demonstrate that a majority of intact axons exhibit remyelination (at least one abnormally short internode, $<100\ \mu m$). Remarkably, shortened internodes were significantly concentrated at the lesion epicenter and individual axons were thinned by 23% compared with their rostral and caudal zones. Mathematical modeling predicted a 25% decrease in conduction velocity at the lesion epicenter due to short internodes and axonal thinning. In conclusion, we do not find a large chronically demyelinated population to target with remyelination therapies. Interventions may be better focused on correcting structural or molecular abnormalities of regenerated myelin.

Introduction

Traumatic spinal cord injury (SCI) induces oligodendrocyte and myelin loss, removing critical support of axonal stability and function (Waxman, 1989; Crowe et al., 1997; Smith and Jeffery, 2006; Rabchevsky et al., 2007; Irvine and Blakemore, 2008; Pohl et al., 2011). Demyelination blocks or severely slows signal conduction through spared axons (Bostock and Sears, 1976; Bostock et al., 1978) and causes "channel spreading"; proteins tightly distributed around nodes of Ranvier, including contactin-associated proteins (CASPRs) and voltage-gated potassium (Kv) channels, disperse along the axolemma (Balentine, 1978; Griffiths and McCulloch, 1983; Nashmi et al., 2000; Karimi-Abdolrezaee et al., 2004). Tight distribution is reestablished with spontaneous remyelination, which begins 2–3 weeks postinjury (McDonald and Ohlrich, 1971; McDonald, 1975; Kakulas, 1999). Regenerated myelin is characterized by abnormally short and thin sheaths (Gledhill et al., 1973a,b; Gledhill and McDonald, 1977), but restores saltatory conduction with near-normal velocity, contributing to functional recovery (Griffiths and McCulloch, 1983; Blight and Young, 1989). How much remyelination occurs and how long spared, demyelinated axons can persist is not clear.

Trophic support provided by myelinating cells is crucial to axon survival in demyelinating disorders (Bjartmar et al., 1999; Lappe-Siefke et al., 2003; Irvine and Blakemore, 2008; Nave, 2010). Yet it is postulated that demyelinated but otherwise intact axons persist chronically in some SCI cases and could be the target for remyelination therapies (Gledhill et al., 1973a; Blight, 1985; Kakulas, 1999; Guest et al., 2005; Totoiu and Keirstead, 2005). This notion is largely based on cross-sectional analysis revealing denuded axons in chronically injured cords. This method does not, however, distinguish between the myelin status of spared, anatomically intact axons and the proximal stumps of injury-severed axons. Distal segments of severed axons undergo protracted Wallerian degeneration and proximal segments persist perilesionally with abortive, dystrophic endbulbs that likely provide no meaningful function (Coleman and Perry, 2002; Guízar-Sahagún et al., 2004; Tom et al., 2004). Previously, we

Received Jan. 1, 2012; revised Feb. 13, 2012; accepted Feb. 20, 2012.

Author contributions: B.E.P., J.L., and P.J.H. designed research; B.E.P., J.L., and J.R.P. performed research; L.S. and S.I.P. contributed unpublished reagents/analytic tools; B.E.P., J.L., J.R.P., L.S., S.I.P., W.T., and P.J.H. analyzed data; B.E.P., J.L., W.T., and P.J.H. wrote the paper.

This work was funded by National Institutes of Health Grants NS046724 (P.J.H.) and NS49447 (S.I.P.), Multiple Sclerosis Society of Canada (W.T.) and the International Foundation for Research on Paraplegia (P.J.H.). P.J.H. is supported by an endowment through Frank and Penny Webster. J.P. is supported by Michael Smith Foundation for Health Research and Canadian Institutes of Health Research doctoral awards. Confocal microscopy was supported in part by the Mike and Lynn Garvey Cell Imaging Laboratory at the University of Washington Institute for Stem Cell and Regenerative Medicine. We thank Dr. J. S. Trimmer (University of California, Davis, CA) for the generous gift of CASPRI antibody and Jie Liu for his help with animal surgeries.

*B.E.P., J.L., and J.R.P. contributed equally to this work.

The authors declare no competing financial interests.

Correspondence should be addressed to Philip J. Horner, University of Washington Department of Neurological Surgery, 815 Mercer Street, Seattle, WA 98109. E-mail: phorner@uw.edu.

DOI:10.1523/JNEUROSCI.0002-12.2012

 0270-6474/12/325120-06$15.00/0

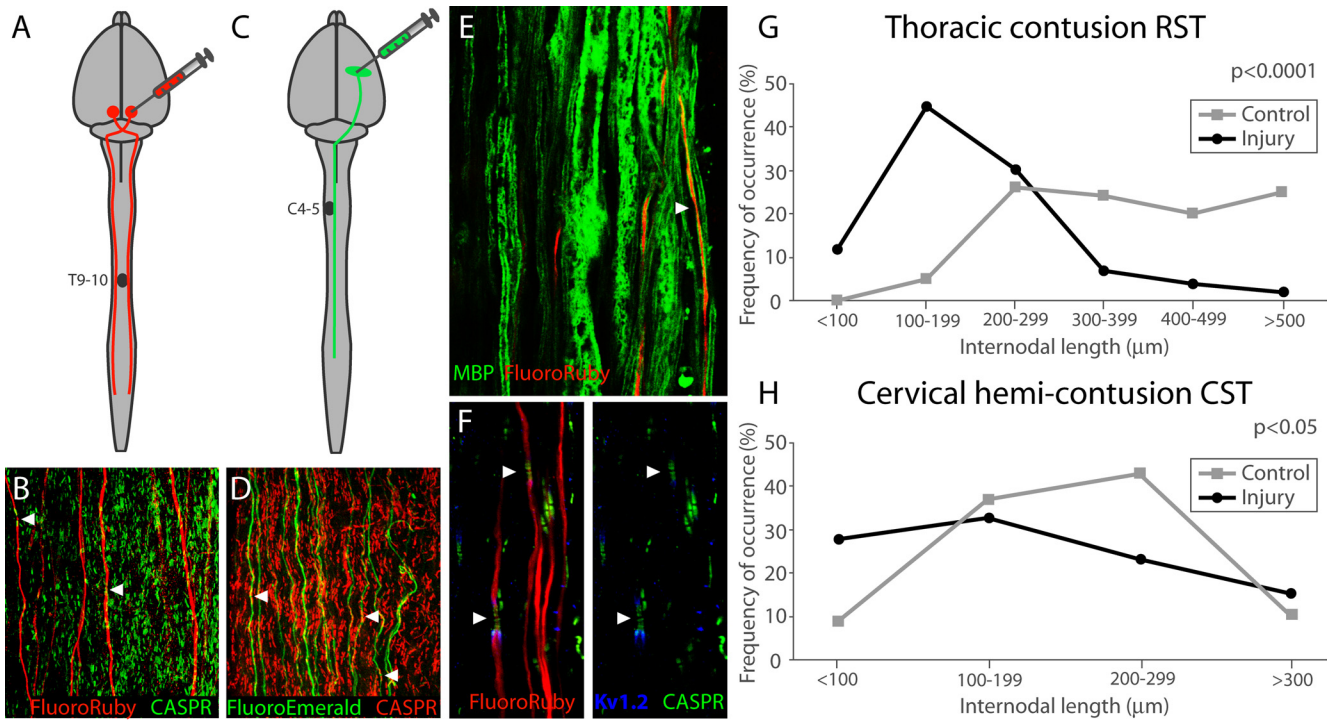

Figure 1. RST and CST anterograde labeling reveal shortened internodes caudal to the injury. ***A–D***, FluoroRuby (***A***) was injected into the red nucleus to trace RST axons (***B***) after thoracic contusion. FluoroEmerald (***C***) was injected into the motor cortex to trace CST axons (***D***) after cervical hemi-contusion. CASPR-labeled paranodes (***B***, ***D***, arrowheads) were used to determine internodal length. ***E***, MBP staining demonstrates that FluoroRuby-labeled axons are myelinated, but probable nodes (arrowhead) are difficult to identify using myelin stains. ***F***, Internodes (arrowheads) are easily identified via immunohistochemical staining. ***G***, ***H***, The distribution of internodal lengths is significantly different between injured and control axons in the RST (***G***) and CST (***H***). Control RST internodes (***G***) are never <100 μm long.

developed an experimental approach to discriminate between severed and spared axons and found in the chronically injured mouse that intact axons are extensively remyelinated (Lasiene et al., 2008). This study challenged whether demyelinated, functionally spared axons persist. However, it did not examine myelin status at the lesion epicenter or in multiple descending tracts. Further, it has been proposed that the mouse model, as opposed to the rat model, has limitations in clinical translation (Inman and Steward, 2003).

To address these issues, we developed methods to determine myelin status and axon diameter of individual descending axons over several intact spinal segments and throughout the lesion epicenter in the rat SCI model. We found for the first time that single spared axons in two tracts critical for locomotion are completely remyelinated, even throughout the injury epicenter, and intact axons do not persist in a demyelinated state following rat SCI.

Materials and Methods

Animals. All procedures were approved by the University of British Columbia, in accordance with the guidelines of the Canadian Council on Animal Care.

Spinal cord injury. Injuries were as described previously (Biernaskie et al., 2007). Adult female rats (280 ± 20 g; Charles River Laboratories) were anesthetized via intraperitoneal injection of ketamine (72 mg/kg; Bioniche) and xylazine (9 mg/kg; Bayer). Thoracic (T) contusion groups ($n = 14$) received T9/10 dorsal laminectomy and contusion injury with 1.3 mm displacement and 6 ms dwell time using The Ohio State University impactor. The unilateral cervical contusion group ($n = 4$) received left C4/C5 dorsal hemi-laminectomy and 1.5 mm spinal cord displacement with a 6 ms dwell (Soblosky et al., 2001; Gensel et al., 2006). Muscle and skin were closed in layers and appropriate postsurgical care administered. Uninjured animals served as controls ($n = 3$).

Anterograde tracing. Thoracic contusion groups received bilateral rubrospinal tract (RST) labeling via stereotaxic medial/lateral red nucleus injections of 0.6 μl of 10% FluoroRuby (tetramethylrhodamine dextran, 10,000 molecular weight (MW), Invitrogen; 6.1/6.1 mm posterior to bregma, 0.75/1.3 mm lateral to midline, 7.0/6.5 mm deep; Fig. 1*B*,*C*). Since thoracic contusion mostly destroys the corticospinal tract (CST), it was labeled in animals receiving unilateral cervical contusion. Right hindpaw and forepaw motor cortex was injected with 10% Fluoroemerald (fluorescein dextran, 10,000 MW; Invitrogen, six 0.4 μl injections; Fig. 1*C*,*D*). The needle was driven 3.2 mm into the cortex at a 30° angle from the dural surface 1.5 mm and 2.5 mm to the right of midline at: 0.3 mm anterior, 0.7 mm posterior and 1.9 mm posterior to bregma. To determine preinjury internode lengths, the left RST and right CST were labeled in age-matched control animals as above.

Tissue processing. Animals received an overdose of chloral hydrate (Sigma) and transcardial perfusion with 0.01 M PBS, then 4% paraformaldehyde 2–3 weeks after tracer injection. Spinal cords were postfixed in 4% paraformaldehyde overnight, then placed in 0.01 M PBS.

Tract teasing and immunohistochemistry. Traced axons were isolated in longitudinal strips using fine forceps under a fluorescent dissecting microscope (Nikon SMZ150). We used two methods to analyze myelin status. First, as described previously (Lasiene et al., 2008), 2 mm strips of labeled RST or CST were created beginning 0.4 mm caudal to the lesion (or at the corresponding spinal level in controls) and incubated for 48 h with primary antibodies, polyclonal CASPR1 (1:100, generous gift from J. S. Trimmer, University of California, Davis, Davis, CA) and monoclonal Kv1.2 (1:200; NeuroMab) or polyclonal myelin basic protein (MBP; 1:200; AbCam) followed by overnight incubation with appropriate secondary Alexa 488, 594, or 647 antibodies (1:250, Invitrogen). Stained tracts were viewed under a Nikon Eclipse TE200 confocal microscope fitted with a Bio-Rad Laser Sharp 2000. Second, we examined myelin status of intact axons at the lesion epicenter and adjacent segments by mechanically teasing labeled RSTs in a continuous strip from 5 mm caudal to 5 mm rostral to the lesion. Teased fibers were immunohisto-

chemically labeled as above and individual axons examined using a Nikon Ti-E inverted microscope with A1 Confocal System.

Quantification. Multiple internodal lengths were measured along axons between CASPR1$^+$ paranodes using NIS Elements and Image-J software. To ensure CASPR1 and Kv1.2 colabel on traced axons, each plane was carefully analyzed in confocal *z*-series. Axon diameters were measured in merged *z*-series.

Statistics. Anatomical data were analyzed using a two-tailed *t* test or one-way ANOVA with Bonferroni post-test for more than two groups. The significance level was $p < 0.05$.

Mathematical modeling. Conduction in spared, intact RST axons was simulated as described previously (Lasiene et al., 2008) using the double cable model of McIntyre et al. (2002) in the NEURON simulation environment (http://senselab.med.yale.edu/senselab/modeldb; Hines and Carnevale, 1997). We constructed three groups of simulated axons using data from RST strips extending 3 mm caudal and rostral to the injury: (1) Conduction properties of 19 individual axons were modeled with experimentally determined internode lengths and axon diameters; (2) The spared RST population was modeled as 100 simulated axons with each internode length picked randomly, with replacement, from either the population of measured internodes within 200 μm of its position for internodes within $\pm$1 mm of the lesion or from all internodes caudal or rostral to the 2 mm lesion for simulated internodes outside the epicenter. Axon diameter reflected the mean injured RST measurement: 1.9 μm within $\pm$1 mm of the lesion center and 2.3 μm distally; (3) Axon diameter was held at 2.3 μm. G-ratio of 0.77 was used for each group (Chomiak and Hu, 2009). Finally, myelin-thinning effects on conduction speed were estimated by repeating Simulation 2 with increased g-ratio. Model axons propagated action potentials in response to a suprathreshold, depolarizing current step delivered to the most rostral node. Internodal conduction velocity was computed as the distance between successive nodes divided by the conduction time. Velocities were smoothed over three successive nodes.

Results

Significantly shorter RST and CST internodes caudal to the lesion

CST and RST axons were filled extensively with tracer (Fig. 1*A–F*). As described previously (Lasiene et al., 2008), we examined axons caudal to the lesion to be sure they were intact: not severed with proximal end bulbs nor their anterograde transport disrupted at the injury epicenter. CASPR1 and Kv1.2 distribution on traced axons was comparable between injured and control animals. We observed no channel spreading (demyelination; Balentine, 1978; Griffiths and McCulloch, 1983; Nashmi et al., 2000; Karimi-Abdolrezaee et al., 2004). Average internodal length on spared, intact RST axons was significantly shorter caudal to the lesion ($p < 0.0001$, mean = 209.2 μm, $n = 143$) compared with uninjured controls (mean = 372.1 μm, $n = 200$; Fig. 1*H*). This 44% decrease in length indicates extensive remyelination (Gledhill and McDonald, 1977). Average injured CST internodal lengths were also significantly shorter ($p < 0.05$, mean = 172.7 μm, $n = 64$) compared with uninjured controls (mean = 207.2 μm, $n = 67$; Fig. 1*I*). This 17% decrease in lengths indicates remyelination of CST axons. However, uninjured CST axons have smaller calibers (CST, 1.379; RST, 2.168; $p < 0.0001$) and substantially shorter internodes than uninjured RST axons, so the relative effect of remyelination—shortened internodes—is not as pronounced. To ensure that injured internode length changes could not be attributed to differences in axonal diameter, we sampled axons of similar diameter in injured and control groups ($p > 0.05$; data not shown). Further, we compared internodal lengths within two populations of RST axons: small (<2 μm) and large (≥ 2 μm) diameter. Internodes were significantly shorter in both groups sampled from injured animals ($p < 0.0001$, mean (<2 μm) = 173.3 μm; mean (≥ 2 μm) = 268.7 μm) compared with noninjured controls ($p < 0.0001$, mean (<2 μm) = 323.7 μm; mean (≥ 2 μm) = 420.5 μm), indicating remyelination across the full range of axonal diameters.

Significantly shorter internodes in the lesion epicenter

To examine myelin status throughout the lesion, we traced ($n = 32$) individual FluoroRuby-labeled RST axons beginning 3 mm caudal to the contusion to ensure they were intact beyond the lesion to 3 mm rostral (Fig. 2*A*). RST axons exhibited significantly shorter average internodal lengths in the 2 mm lesion epicenter (mean = 231.1 μm, $n = 226$) compared with the 2 mm caudal ($p < 0.001$, mean = 323.5 μm, $n = 73$) and rostral ($p < 0.05$, mean = 292.4, $n = 54$; Fig. 2*B–D*,*F*,*G*). T10–11 RST internodal lengths in uninjured controls were never <100 μm (Fig. 1*G*), whereas 53% of injured axons had at least one internode <100 μm, indicating that a majority of spared RST axons were affected by injury-induced myelin remodeling. Furthermore, 80% of internodes <100 μm lay within the 2 mm lesion epicenter, suggesting that the majority of remyelination events occur there (Fig. 2*G*). In each prepared strip, a large population of severed axons was visible rostral to the lesion, identified by their characteristic dystrophic end bulbs (Fig. 2*A*). Only these cut axons exhibited evidence of channel spreading, with heavy misdistribution of CASPR1 and Kv1.2 to their endbulbs (Fig. 2*D*,*E*).

Significantly reduced average axon diameters and individual axon thinning at the lesion epicenter

Extensive RST FluoroRuby labeling allowed reliable axon diameter measurement within randomly selected T10–11 strips (caudal to injury). Injured axon diameters were significantly smaller ($p < 0.0001$, *t* test, one-tail, mean = 1.81 μm) than controls (mean = 2.37 μm; Fig. 2*H*). This 24% decrease in average axonal diameter is similar to previous reports (Nashmi and Fehlings, 2001). Frequency of large diameter axons (>2.5 μm) significantly decreased whereas medium caliber (1.5–2.5 μm) occurrence increased with injury. Last, we measured axon diameter at three locations along individual RST axons traced throughout the extent of the lesion. Axons >2 μm in diameter caudal and rostral to the lesion, but not those <2 μm in diameter, were thinned by 23% on average at the lesion epicenter ($p < 0.05$; Fig. 2*I*), demonstrating again that larger caliber axons are preferentially affected by injury.

Short internodes and thinned axons slow conduction velocity through the lesion

Previously, we reported a 32% reduction in conduction velocity in axons simulated with data from remyelinated versus uninjured mouse RST axons (Lasiene et al., 2008). Here, we used the same mathematical model to simulate conduction through the lesion epicenter. No conduction failure occurred. However, conduction velocity in individual injured axons was significantly reduced through the lesion (Fig. 2*J–L*). Shortened internodal lengths reduced average conduction velocity through the 2 mm lesion center by 7% compared with rostral zones (13.7 vs 12.7 m/s, $p < 0.001$). Thinned axon diameters in the lesion epicenter compounded the effect; the combination of shortened internodes and thinned axon caliber reduced average conduction velocity by 25% through the lesion (10.2 m/s, $p < 0.001$). Although myelin thickness was not measured in this study, it is known that remyelination produces thin myelin (Gledhill et al., 1973a; Totoiu and Keirstead, 2005; Lasiene et al., 2008). Conduction velocity through the 2 mm lesion center was decreased an additional 2%, relative to rostral zones, in simulated axons with a 5% increase in

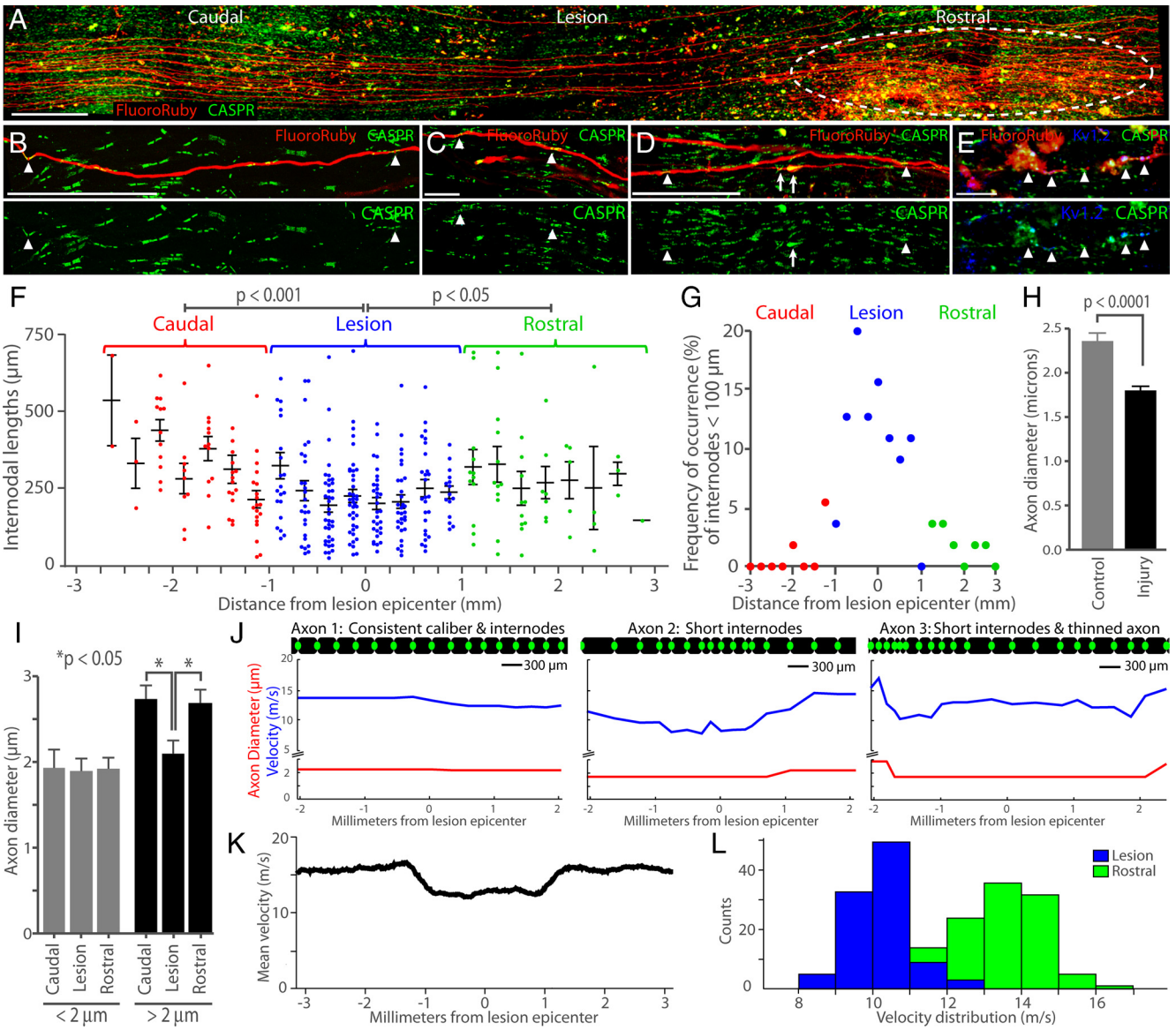

Figure 2. Channel spreading is evident on severed axons; intact axons exhibit thinning and short internodes concentrated at the lesion epicenter. ***A***, Example of isolated FluoroRuby labeled RST axons in stitched confocal *z*-series (merged) centered on the lesion epicenter. Dystrophic endbulbs of cut axons are visible rostral to the epicenter (white dashed circle). ***B***, A 212 μm internode caudal to the injury, delineated by arrowheads. ***C***, A 68 μm internode at the lesion epicenter. ***D***, Arrowheads delineate a 233 μm internode on an intact axon rostral to injury; white arrows highlight channel spreading on an axon severed after the image edge. ***E***, Severed axons exhibit dystrophic endbulbs with heavy mislocalization of CASPR1 and Kv1.2 protein (arrowheads). Scale bars: ***A***, 500 μm; ***B***, ***D***, 100 μm; ***C***, ***E***, 25 μm. ***F***, All measured internode lengths plotted by the distance of the center of the internode from the lesion epicenter. Short internodes are significantly concentrated within the 2 mm center of the lesion (blue dots). ***G***, The distribution of internodes shorter than 100 μm across the lesion demonstrates a high concentration at the epicenter (blue dots). ***H***, Average RST axon diameter was reduced by injury. ***I***, Axon diameters of individual large-bore axons were thinned at the lesion epicenter compared with rostral and caudal zones. ***J–L***, Conduction velocity of simulated RST axons. ***J***, Velocity (blue) between nodes simulated with data from three examples of real, labeled axons; axon diameter (red) and internode length (axon diagrams shown to scale: black, myelin; green dot, node). Axon 1 exhibited little variation in internode length, axon diameter, and conduction velocity. Axon 2 exhibited short internodes at the lesion epicenter and reduced conduction velocity. Axon 3 exhibited short internodes, axon diameter, and reduced conduction velocity. ***K***, Average velocity between nodes for 100 simulated axons constructed from all measured internode lengths and axon diameters; shortened internodes and axon thinning reduced conduction speed at the lesion epicenter. ***L***, Distributions of conduction velocities through 2 mm regions centered at the lesion (blue) and rostral to the lesion (green); velocities are significantly reduced ($p \ll 0.001$) within the lesion.

G-ratio (based on RST data from Lasiene et al., 2008) in the lesion zone. Thus, reduced axon diameter has a more significant effect on conduction through the lesion epicenter than changes in internode length or myelin thickness.

Discussion

Extending previous work (Lasiene et al., 2008), these data directly challenge the existence of spared, intact axons with chronic demyelination, but importantly, do not refute the presence of chronic demyelination per se. We and others report small populations of degenerating and severed axons with denuded segments, even a decade after SCI in rare human cases (Gledhill et al., 1973a; Guest et al., 2005; Totoiu and Keirstead, 2005; Lasiene et al., 2008). However, our data do not support chronic persistence of a large target population of intact axons for remyelination therapies. Instead, we demonstrate robust endogenous remyelination following SCI in rats where lesion characteristics closely resemble human injuries.

Similar to previous studies, we found a 24% decrease in axonal diameter after injury (Blight, 1983; Nashmi and Fehlings, 2001). It is unclear whether large diameter axons preferentially die due

to traumatic insult or shrink due to initial demyelination or incomplete remyelination. Large caliber axons have higher metabolic and trophic requirements that could render them more vulnerable to injury (Blight and Decrescito, 1986; Blight, 1991). Alternatively, the relationship between myelin thickness and axon diameter could be calibrated to a new postinjury setting. Intriguingly, we found individual large caliber axons were 23% thinner at the lesion epicenter where the incidence of shortened internodes was highest. This raises the possibility that abnormal myelination could decrease axon caliber in a segment-by-segment fashion. How myelin-derived signals control axon size is not clear, but it has been demonstrated that axon caliber is increased by proper myelination during development (Hsieh et al., 1994; Sánchez et al., 1996) and is reduced in dysmyelinated mice null for crucial myelin proteins (de Waegh et al., 1992; Brady et al., 1999).

Our data provide novel insight into this phenomenon. Many studies demonstrate remyelination following SCI (Bunge et al., 1961; Gledhill et al., 1973a; Smith and Jeffery, 2006), but the extent reported here, affecting at least 53% of spared RST axons, represents a previously underappreciated level of endogenous myelin regeneration, and therefore abnormal myelin. An optimal physiological ratio between axon diameter and myelin length and thickness is thought to exist to ensure effective conduction velocity (Waxman, 1980). Together, shortened internodes, thinned myelin, and axon caliber reduced conduction velocity through the lesion epicenter in simulated axons.

Conclusion

By assessing multiple quantitative measures of axons and myelin, these data refine our understanding of the underlying causes of conduction slowing in chronic SCI away from frank demyelination and toward more subtle qualities of regenerated myelin. Enhancing its length or thickness could have therapeutic value. Although attempts to use developmental pathways to this end have reportedly failed (Harrington et al., 2010), much remains to be explored about the regulation of regenerated myelin parameters. Future studies should be directed toward better understanding the timing and causes of axon and myelin degeneration to optimally define therapeutic targets for treating neural trauma, demyelinating disease, and aging.

References

Balentine JD (1978) Pathology of experimental spinal cord trauma. I. The necrotic lesion as a function of vascular injury. Lab Invest 39:236–253.

Biernaskie J, Sparling JS, Liu J, Shannon CP, Plemel JR, Xie Y, Miller FD, Tetzlaff W (2007) Skin-derived precursors generate myelinating Schwann cells that promote remyelination and functional recovery after contusion spinal cord injury. J Neurosci 27:9545–9559.

Bjartmar C, Yin X, Trapp BD (1999) Axonal pathology in myelin disorders. J Neurocytol 28:383–395.

Blight AR (1983) Axonal physiology of chronic spinal cord injury in the cat: intracellular recording in vitro. Neuroscience 10:1471–1486.

Blight AR (1985) Delayed demyelination and macrophage invasion: a candidate for secondary cell damage in spinal cord injury. Cent Nerv Syst Trauma 2:299–315.

Blight AR (1991) Morphometric analysis of a model of spinal cord injury in guinea pigs, with behavioral evidence of delayed secondary pathology. J Neurol Sci 103:156–171.

Blight AR, Decrescito V (1986) Morphometric analysis of experimental spinal cord injury in the cat: the relation of injury intensity to survival of myelinated axons. Neuroscience 19:321–341.

Blight AR, Young W (1989) Central axons in injured cat spinal cord recover electrophysiological function following remyelination by Schwann cells. J Neurol Sci 91:15–34.

Bostock H, Sears TA (1976) Continuous conduction in demyelinated mammalian nerve fibers. Nature 263:786–787.

Bostock H, Sherratt RM, Sears TA (1978) Overcoming conduction failure in demyelinated nerve fibres by prolonging action potentials. Nature 274:385–387.

Brady ST, Witt AS, Kirkpatrick LL, de Waegh SM, Readhead C, Tu PH, Lee VM (1999) Formation of compact myelin is required for maturation of the axonal cytoskeleton. J Neurosci 19:7278–7288.

Bunge MB, Bunge RP, Ris H (1961) Ultrastructural study of remyelination in an experimental lesion in adult cat spinal cord. J Biophys Biochem Cytol 10:67–94.

Chomiak T, Hu B (2009) What is the optimal value of the g-ratio for myelinated fibers in the rat CNS? A theoretical approach. PLoS One 4:e7754.

Coleman MP, Perry VH (2002) Axon pathology in neurological disease: a neglected therapeutic target. Trends Neurosci 25:532–537.

Crowe MJ, Bresnahan JC, Shuman SL, Masters JN, Beattie MS (1997) Apoptosis and delayed degeneration after spinal cord injury in rats and monkeys. Nat Med 3:73–76.

de Waegh SM, Lee VM, Brady ST (1992) Local modulation of neurofilament phosphorylation, axonal caliber, and slow axonal transport by myelinating Schwann cells. Cell 68:451–463.

Gensel JC, Tovar CA, Hamers FP, Deibert RJ, Beattie MS, Bresnahan JC (2006) Behavioral and histological characterization of unilateral cervical spinal cord contusion injury in rats. J Neurotrauma 23:36–54.

Gledhill RF, McDonald WI (1977) Morphological characteristics of central demyelination and remyelination: a single-fiber study. Ann Neurol 1:552–560.

Gledhill RF, Harrison BM, McDonald WI (1973a) Demyelination and remyelination after acute spinal cord compression. Exp Neurol 38:472–487.

Gledhill RF, Harrison BM, McDonald WI (1973b) Pattern of remyelination in the CNS. Nature 244:443–444.

Griffiths IR, McCulloch MC (1983) Nerve fibres in spinal cord impact injuries. Part 1. Changes in the myelin sheath during the initial 5 weeks. J Neurol Sci 58:335–349.

Guest JD, Hiester ED, Bunge RP (2005) Demyelination and Schwann cell responses adjacent to injury epicenter cavities following chronic human spinal cord injury. Exp Neurol 192:384–393.

Guízar-Sahagún G, Grijalva I, Salgado-Ceballos H, Espitia A, Orozco S, Ibarra A, Martínez A, Franco-Bourland RE, Madrazo I (2004) Spontaneous and induced aberrant sprouting at the site of injury is irrelevant to motor function outcome in rats with spinal cord injury. Brain Res 1013:143–151.

Harrington EP, Zhao C, Fancy SP, Kaing S, Franklin RJ, Rowitch DH (2010) Oligodendrocyte PTEN is required for myelin and axonal integrity, not remyelination. Ann Neurol 68:703–716.

Hines ML, Carnevale NT (1997) The NEURON simulation environment. Neural Comput 9:1179–1209.

Hsieh ST, Kidd GJ, Crawford TO, Xu Z, Lin WM, Trapp BD, Cleveland DW, Griffin JW (1994) Regional modulation of neurofilament organization by myelination in normal axons. J Neurosci 14:6392–6401.

Inman DM, Steward O (2003) Physical size does not determine the unique histopathological response seen in the injured mouse spinal cord. J Neurotrauma 20:33–42.

Irvine KA, Blakemore WF (2008) Remyelination protects axons from demyelination-associated axon degeneration. Brain 131:1464–1477.

Kakulas BA (1999) A review of the neuropathology of human spinal cord injury with emphasis on special features. J Spinal Cord Med 22:119–124.

Karimi-Abdolrezaee S, Eftekharpour E, Fehlings MG (2004) Temporal and spatial patterns of Kv1.1 and Kv1.2 protein and gene expression in spinal cord white matter after acute and chronic spinal cord injury in rats: implications for axonal pathophysiology after neurotrauma. Eur J Neurosci 19:577–589.

Lappe-Siefke C, Goebbels S, Gravel M, Nicksch E, Lee J, Braun PE, Griffiths IR, Nave KA (2003) Disruption of Cnp1 uncouples oligodendroglial functions in axonal support and myelination. Nat Genet 33:366–374.

Lasiene J, Shupe L, Perlmutter S, Horner P (2008) No evidence for chronic demyelination in spared axons after spinal cord injury in a mouse. J Neurosci 28:3887–3896.

McDonald WI (1975) Mechanisms of functional loss and recovery in spinal cord damage. Ciba Found Symp 34:23–33.

McDonald WI, Ohlrich GD (1971) Quantitative anatomical measurements on single isolated fibres from the cat spinal cord. J Anat 110:191–202.

Mclntyre CC, Richardson AG, Grill WM (2002) Modeling the excitability of

mammalian nerve fibers: influence of afterpotentials on the recovery cycle. J Neurophysiol 87:995–1006.

Nashmi R, Fehlings MG (2001) Changes in axonal physiology and morphology after chronic compressive injury of the rat thoracic spinal cord. Neuroscience 104:235–251.

Nashmi R, Jones OT, Fehlings MG (2000) Abnormal axonal physiology is associated with altered expression and distribution of Kv1.1 and Kv1.2 K+ channels after chronic spinal cord injury. Eur J Neurosci 12:491–506.

Nave KA (2010) Myelination and support of axonal integrity by glia. Nature 468:244–252.

Pohl HB, Porcheri C, Mueggler T, Bachmann LC, Martino G, Riethmacher D, Franklin RJ, Rudin M, Suter U (2011) Genetically induced adult oligodendrocyte cell death is associated with poor myelin clearance, reduced remyelination, and axonal damage. J Neurosci 31:1069–1080.

Rabchevsky AG, Sullivan PG, Scheff SW (2007) Temporal-spatial dynamics in oligodendrocyte and glial progenitor cell numbers throughout ventrolateral white matter following contusion spinal cord injury. Glia 55:831–843.

Sánchez I, Hassinger L, Paskevich PA, Shine HD, Nixon RA (1996) Oligodendroglia regulate the regional expansion of axon caliber and local accumulation of neurofilaments during development independently of myelin formation. J Neurosci 16:5095–5105.

Smith PM, Jeffery ND (2006) Histological and ultrastructural analysis of white matter damage after naturally-occurring spinal cord injury. Brain Pathol 16:99–109.

Soblosky JS, Song JH, Dinh DH (2001) Graded unilateral cervical spinal cord injury in the rat: evaluation of forelimb recovery and histological effects. Behav Brain Res 119:1–13.

Tom VJ, Steinmetz MP, Miller JH, Doller CM, Silver J (2004) Studies on the development and behavior of the dystrophic growth cone, the hallmark of regeneration failure, in an in vitro model of the glial scar and after spinal cord injury. J Neurosci 24:6531–6539.

Totoiu MO, Keirstead HS (2005) Spinal cord injury is accompanied by chronic progressive demyelination. J Comp Neurol 486:373–383.

Waxman SG (1980) Determinants of conduction velocity in myelinated nerve fibers. Muscle Nerve 3:141–150.

Waxman SG (1989) Demyelination in spinal cord injury. J Neurol Sci 91:1–14.